Electronic Supplementary Material (ESI) for ChemComm.

Supporting Information

Lipid phase dependent distinct emission behaviour of hydrophobic carbon dots: C-dots based membrane probe

1 Materials and Methods:

1.1 Materials:

All the phospholipids, namely, DPPC (1,2-dipalmitoyl-sn-glycero-3-phosphocholine), DMPC (1,2-dimyristoyl-sn-glycero-3-phosphocholine), DOPC (1,2-dioleoyl-sn-glycero-3-phosphocholine) and DMPG (1,2-dimyristoyl-sn-glycero-3-phospho-(1'-rac-glycerol) (sodium salt)) were purchased from Avanti polar lipids. The chemical structures of these lipids are shown in **scheme S1**. The other chemicals melamine, dithiosalicylic acid (DTSA), o-Phenylenediamine, Citric acid, 1-(2-pyridylazo)-2-naphthol (PAN), L-phenylalanine (L-Phe), L-tryptophan (L-Trp), Calcium chloride ($CaCl_2$) and Indium chloride ($InCl_3$) were purchased from Sigma-Aldrich. All these chemicals were used without any further purification. All the solvents i.e. acetic acid, ethanol, DMF, chloroform, acetone, methanol, and ethylene glycol used in the experiments were of the spectroscopic grade obtained from Merck. Milli-Q water was used to prepare all of the lipid vesicles solutions.

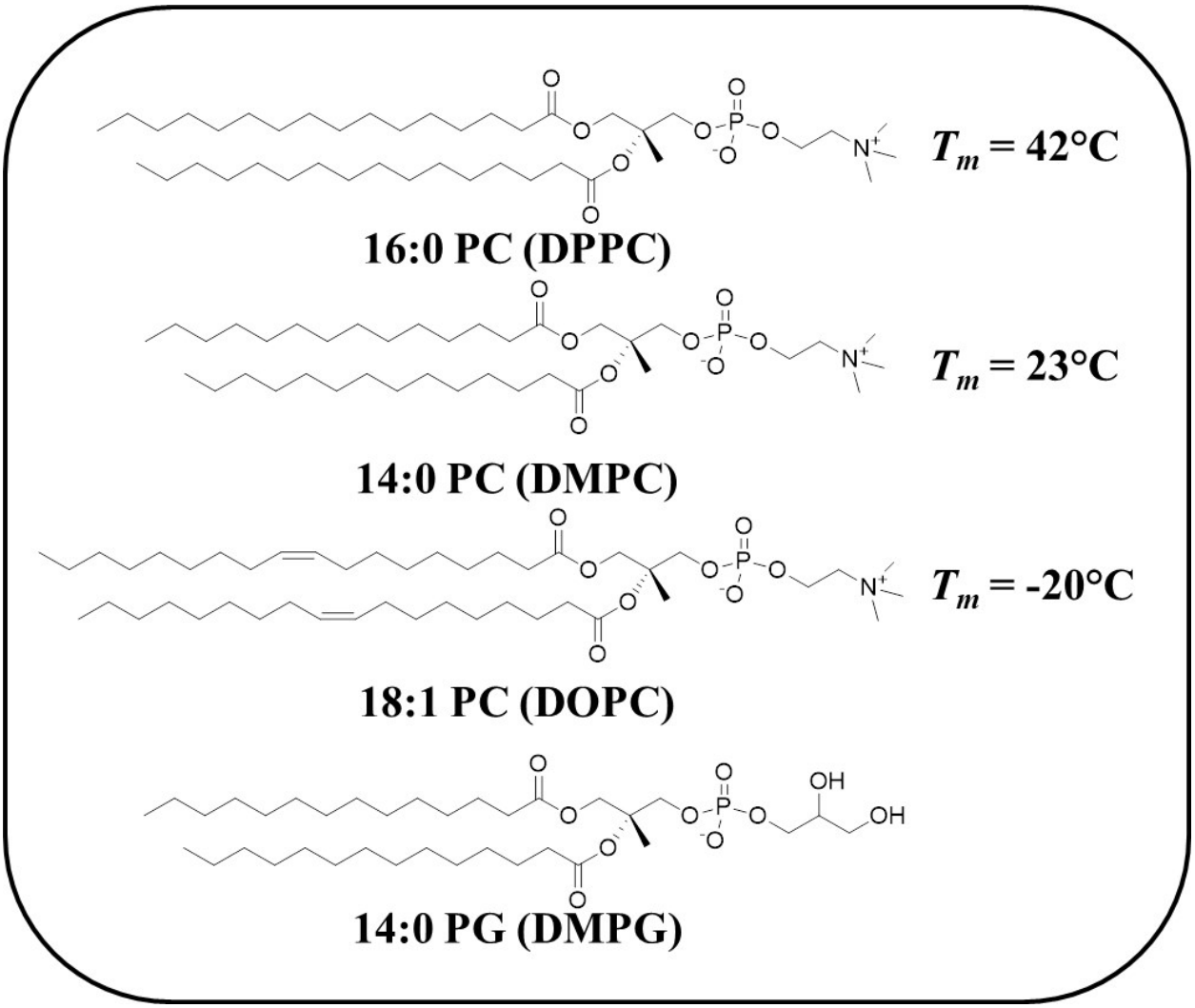

Scheme S1: Chemical structures of the DPPC, DMPC, DOPC and DMPG.

1.2 Preparation of Hydrophobic carbon dots (H-CDs):

The hydrophobic carbon dots were prepared by the previously reported method.[1]Briefly, 100.8 mg melamine and 272 mg dithiosalicylic acids were dissolved into 20 mL acetic acid with ultrasonic treatment and then the solution was transferred into a 40 mL Teflon-lined autoclave and kept at 180 °C for 8 h in an air oven. After the solvothermal treatment, the as-prepared H-CD solution was added to 500 ml of boiled water to form H-CD powder and washed out the residual raw materials and solvent. Finally, purified H-CD powder was achieved through vacuum filtration.

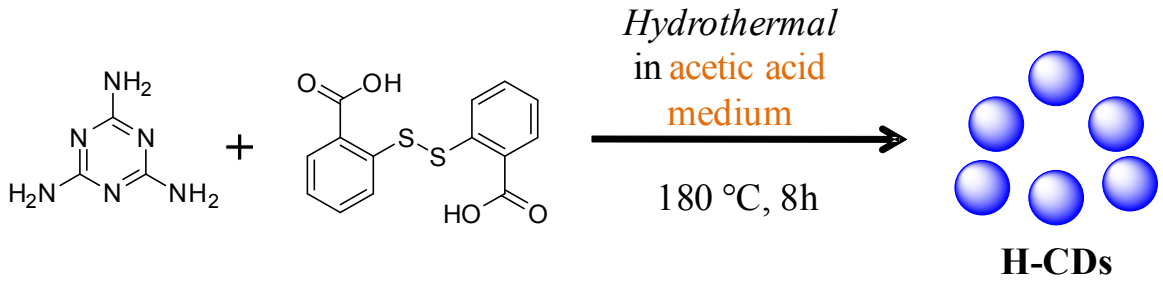

Scheme S2: Schematic representation of the synthesis procedure of the H-CDs.

1.3 Preparation of carbon dots (o-CDs) from o-Phenylenediamine:

Ortho-phenylenediamine (0.2 g) was dissolved in 20 mL of Mili-Q water, and the solution was transferred into a 40 mL Teflon-lined autoclave and heated at 180 °C for 12 h, as reported previously.[2-3] Following cooling down to room temperature, the as synthesized dark yellow solution was centrifuged to 8000 rpm and filter against 0.2 µm filter to remove the larger aggregates. Finally, the solution was freeze-drying and kept under high-vacuum to get the yellow color powder o-CDs.

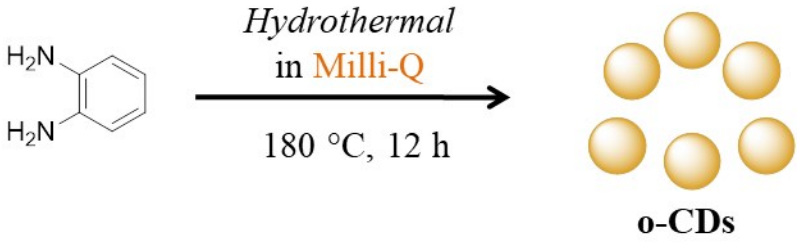

Scheme S3: Schematic illustration for the preparation processes of multicolor o-CDs.

1.4 Preparation of multicolor carbon dots (M-CDs):

M-CDs were synthesized by a previously reported simple solvothermal method.[4] Citric acid (CA, 1.15 g) and PAN (0.07 g) was dissolved in 30 mL ethanol by ultrasonication. Then the mixture was transferred into a 40 mL Teflon-lined autoclave and heated at 200 °C for 7 h. Then, the as synthesized dispersion was filtered by using a microporous membrane (0.2 µm) to remove the larger particles. The excess ethanol was removed by using rotary evaporator and freeze-dried to obtain viscous solids M-CDs for further use.

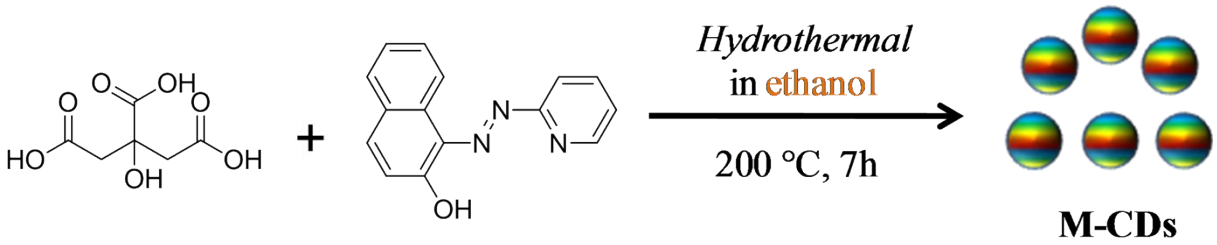

Scheme S4: Schematic illustration for the preparation processes of multicolor M-CDs.

1.5 Preparation of lipid-CD assemblies:

H-CD embedded lipid vesicles or lipid-CD assemblies (DMPC-CD, DPPC-CD, DOPC-CD and DMPC/DMPG-CD) were prepared by hydration of dried Lipid-CD thin-films. The ratio of zwitterionic and charged lipid was fixed at 8:2 for preparing the DMPC/DMPG-CD assemblies. The required amount of lipids and H-CDs were dissolved in a mixture of chloroform and ethanol, and then the solvents were removed completely in a rotary evaporator. The flask containing a dry lipid film was placed under a high vacuum overnight to remove any residual solvent. The film was hydrated with a preheated Milli-Q, vortex for 5 minutes and stirred for 30 minutes above the phase transition of the respective lipid and these cycles were repeated for 3 times. The final concentration of lipid and H-CDs were 1 mM and 50 µg mL^{-1} respectively. The o-CD and M-CD based lipid-CD assemblies were also prepared by using the same above mentioned protocol.

2 Instrumentation:

2.1 Steady-State Fluorescence Measurements:

Steady-state fluorescence spectra were recorded using a Fluoromax-4p spectrofluorometer from Horiba Jobin Yvon (model: FM-100). The excitation and emission slits were 2/2 for all the emission measurements. We maintained temperature (T) at 25°C throughout all the experiments, otherwise, we mentioned the temperature. The fluorescence quantum yield (QY) was estimated relative to Quinine Sulfate (Φ_{ST}) in water medium by using the following equation:

$$\Phi_S = \Phi_{ST}\left(\frac{I_S}{I_{ST}}\right)\left(\frac{\eta_S^2}{\eta_{ST}^2}\right)\left(\frac{A_{ST}}{A_S}\right) \quad (1)$$

Here, Φ is the QY, I is the integrated fluorescence intensity, η is the refractive index of the solvent, and A is the optical density. The subscript "ST" stands for standard and "S" stands for the samples.

2.2 Time-Resolved Fluorescence Measurements:

For lifetime measurements, we used a picosecond TCSPC (time-correlated single-photon counting) machine from Horiba (Fluorocube-01-NL).We used a filter on the emission side to eliminate the scattered light. The signals were collected at magic angle (54.75°) polarization using a photomultiplier tube (TBX-07C) as a detector with instrument response function ~560 ps. The data analysis was performed using IBH DAS Version 6 decay analysis software.

The decays were fitted with a multi-exponential function.

$$D(t) = \sum_{i=1}^{n} a_i exp(\frac{-t}{\tau_i}) \qquad (2)$$

Here D(t) denotes normalized fluorescence decay and a_i is the normalized amplitude of decay components τ_i, respectively. The quality of the fit was judged by reduced chi-square (χ^2) values and corresponding residual distribution. The acceptable fit has a χ^2 near unity.

For the anisotropy decays, the same setup and a motorized polarizer were used in the emission side. The emission intensities at parallel and perpendicular polarizations were collected alternatively until a certain peak difference between parallel and perpendicular decay was achieved. The same software was also used to analyze the anisotropy data. The time-resolved anisotropy decay was described with the following equation:

$$r(t) = \frac{I_{\parallel}(t) - GI_{\perp}(t)}{I_{\parallel}(t) + 2GI_{\perp}(t)} \qquad (3)$$

Where *r(t)* is the rotational relaxation correlations function, $I_{\parallel}(t)$ and $I_{\perp}(t)$ are the parallel and perpendicular components of the fluorescence and G is the correlation factor.

2.3 Confocal microscopy:

For the confocal imaging of samples, we used a confocal microscope from OLYMPUS, model no. IX-83. A Multiline Ar laser (gas laser) with an excitation wavelength of 405 nm was used to

study the lipid-CD assemblies. The emission was collected by using three emission filter i. e. emission filter EM 410/480 for the blue region, emission filter EM 490/560 for the green region, and emission filter EM 575/650 nm for the red region. An aliquot of the freshly prepared sample by the previous describe method was immobilized on a clean cover slide and kept in a vacuum desiccator to remove the solvent. Then the sample containing the cover slide was fixed by a glass slide in a sandwich manner by using transparent nail polish before imaging.

2.4 High resolution-Transmission electron microscopy (HR-TEM):

High-resolution transmission electron microscopy images were taken by using a field emission gun transmission electron microscope (Model: Tecnai G2, F30) with an acceleration voltage of 300 kV. The diluted solutions of the samples were dried on a carbon-coated copper grid by slow evaporation in the air at room temperature before measurements.

2.5 Fourier transformed infrared (FT-IR) and X-ray Photoelectron Spectroscopy (XPS) measurement:

The FT-IR spectra of powder samples were obtained by using a Perkin Elmer Spectrum 2 model. The XPS measurements were conducted with a Shimadzu, Axis Supra X-ray photoelectron spectrometer. Spectra were acquired using the Al-Kα monochromatic X-ray source (1,486.7 eV) with 0° take of angle (normal to analyzer). The vacuum pressure in the analyzing chamber was maintained at ~4.8$\times$10^{-9} Torr during the acquisition process. The survey spectra were collected with pass energy 80 eV, and 1.0 eV step size, dwell time 100 ms. High resolution XPS spectra were collected for C 1s, N 1s, O 1s, and S 2p, with pass energy 80 eV and 0.1 eV step size, dwell time 299 ms. All binding energies were corrected by using the contaminant carbon (C 1s = 284.8 eV) as an internal standard.

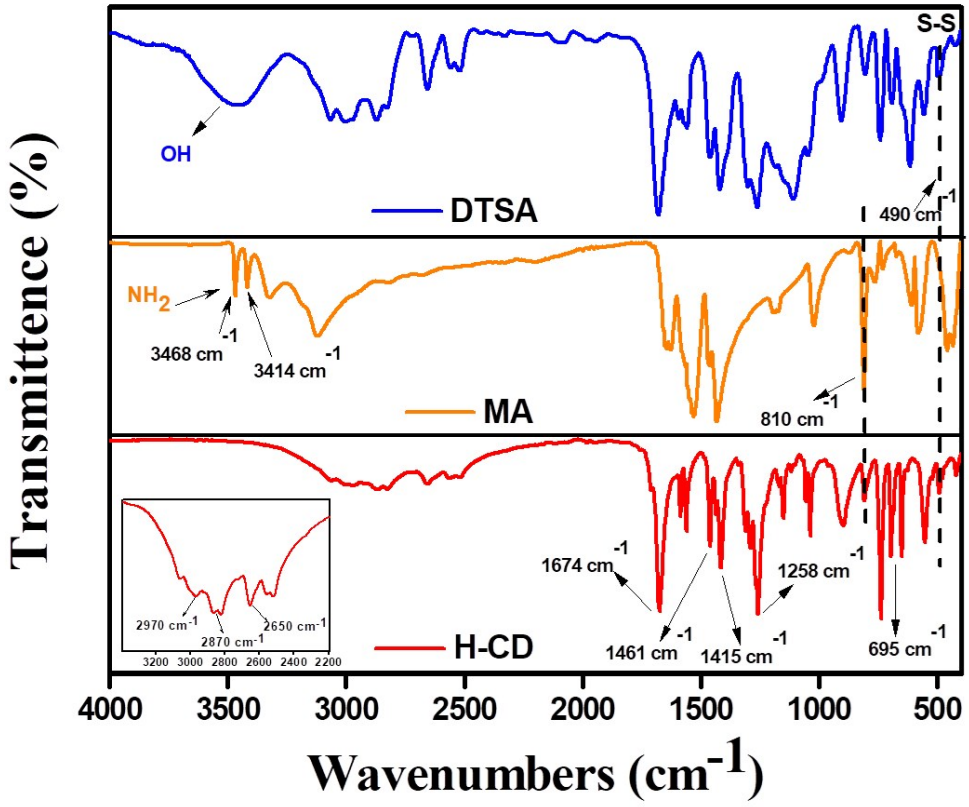

Figure S1: FT-IR spectrum of dithiosalicylic acid (DTSA), melamine (MA) and the H-CDs.

Discussion: The Fourier transformed infrared (FT-IR) spectra reveals that that the surface of the H-CD contains S-S (490 cm^{-1}), C-S (695 cm^{-1}), S-H (2650 cm^{-1}), methylene (2870 cm^{-1} and 2970 cm^{-1}), C=C (1461 cm^{-1}), amide carbonyl (1674 cm^{-1}), C-N (1415 cm^{-1}) and aromatic C-N (1258 cm^{-1}) functional groups, which is good agreement with the Yang et. Al.[1] We also observed that, the FT-IR spectra of the MA exhibit a peak at 3468-3414 cm^{-1} which correspond to the hydrophilic amino group and DTSA exhibit a peak at 3467 cm^{-1} which correspond to the hydrophilic hydroxyl group. However, after the carbonization and amidation, the hydrophilic amino groups of MA and hydroxyl group of DTSA are disappearing completely in the H-CDs, which possibly contribute the hydrophobic property of the H-CDs.

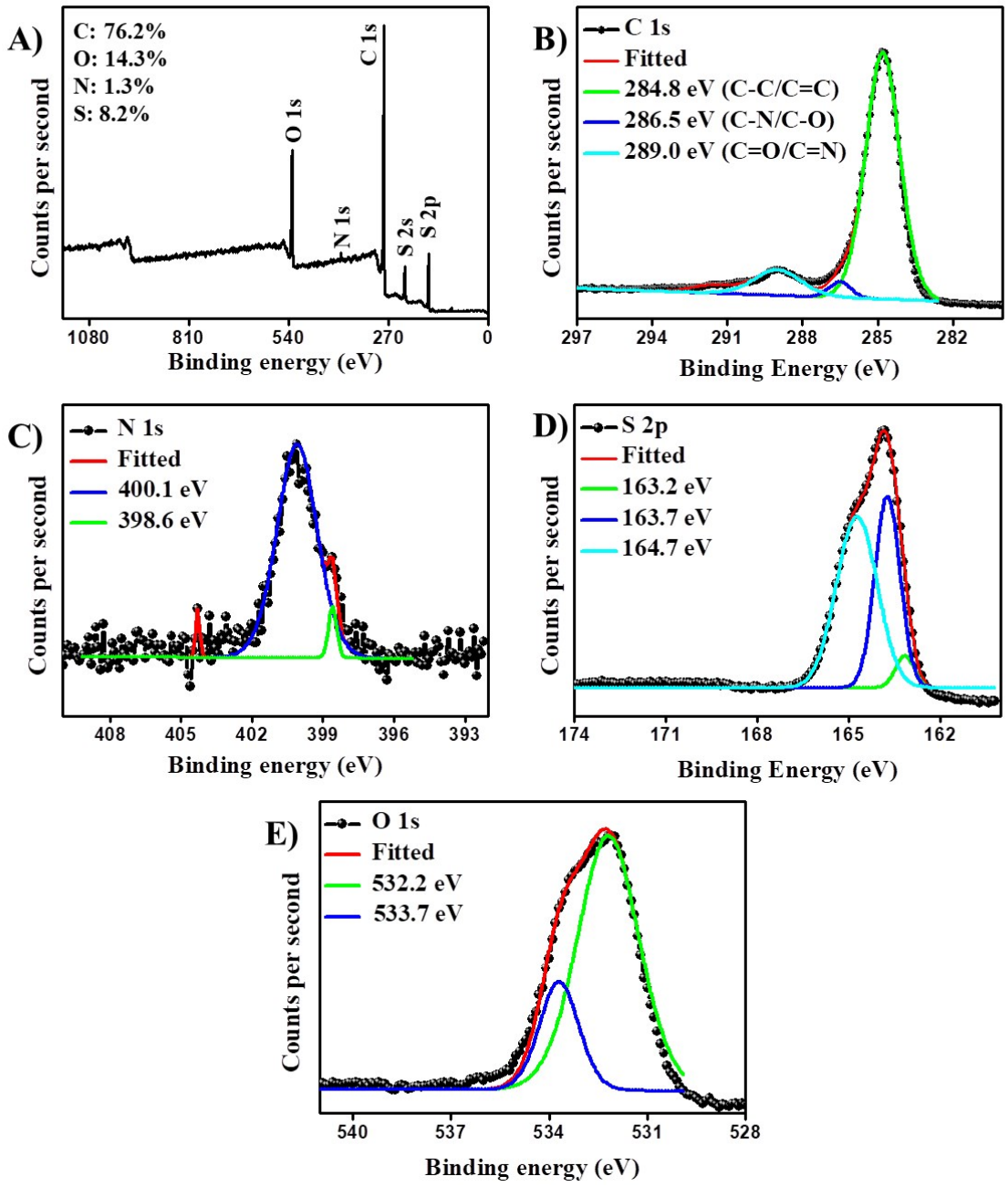

Figure S2: A) XPS spectrum and high-resolution B) C 1s, C) N 1s, D) S 2p, and E) O 1s spectra of the H-CDs.

Discussion: The full XPS spectra in figure S4 display five typical peaks at 163.8, 227.2, 284.8, 399.8 and 531.8 eV for S 2p, S 2s, C 1s, N 1s, and O 1s, respectively. Suggesting that H-CDs contains C, N, O, and S element and their atomic ratio was found 76.2%, 1.3%, 14.3% and 8.2% respectively. The high resolution XPS spectrum of C 1s band was deconvoulated into three binding energy peak, 284.8, 286.5 and 289.0 eV, which are assigned to the C-C/C=C, C-N and C=O/C=N, respectively. The O 1s spectra contain two peak 532.2 and 533.7 eV for C=O and C-OH/C-O-C band, respectively. The N 1s band exhibit two peaks at 398.6 and 400.1 eV, respectively, which is assigned to the pyridinic C3-N and pyrrolic C2-N-H groups. The S 2p band in figure S2D shows three peaks at 163.2, 163.7 and 164.7 eV which correspond to the S-C, S-H, and S-S respectively. Therefore, we conclude that, H-CD possesses graphite-like core with defects caused by nitrogen atoms and disulfide bonds and the surface of the H-CDs covered with C, N, O and S containing heterocycles.

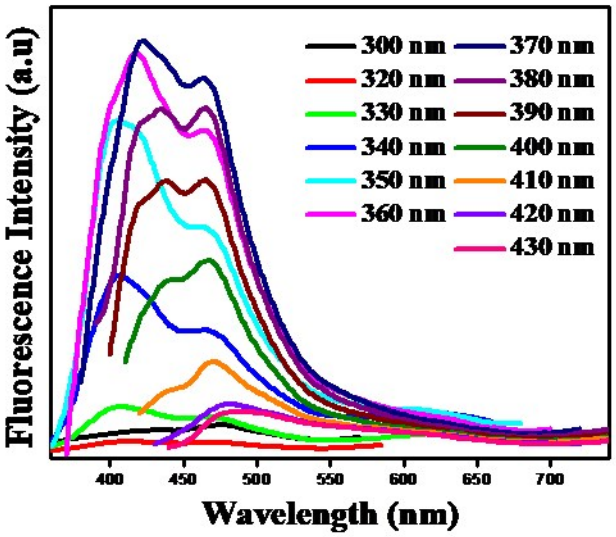

Figure S3: Excitation-dependent emission spectra of the as-synthesized H-CDs in acetic acid solutions.

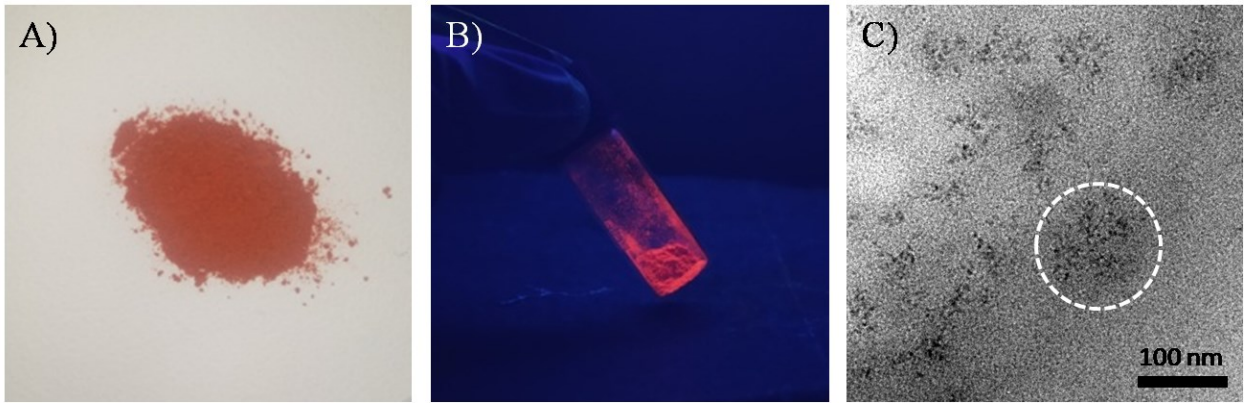

Figure S4: Images of the aggregated H-CDs A) in sunlight, B) under 365 nm UV lamp, and C) in HR-TEM.

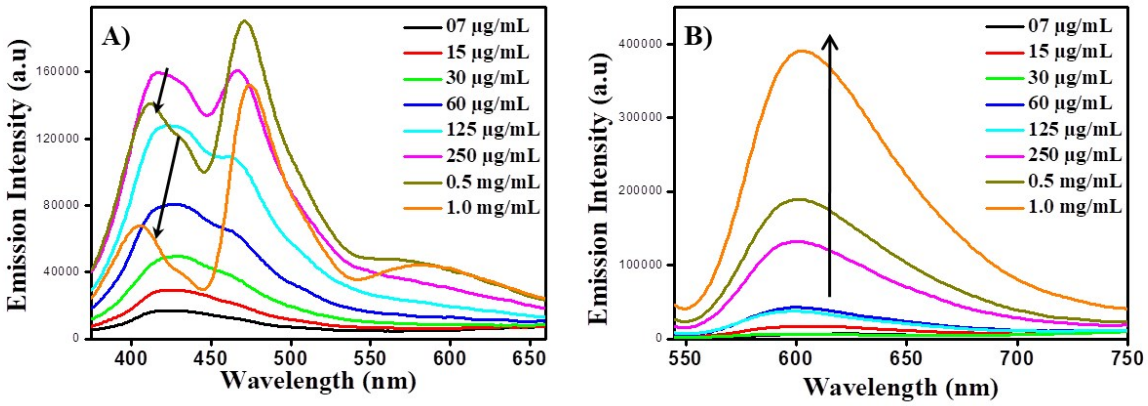

Figure S5: Concentration dependent emission of the H-CDs at the blue and red region in A) acetic acid and B) water medium respectively.

Discussion: Concentration dependent emission of the H-CDs were also studied in both blue and red region (in acetic acid and water medium respectively) to get insight into the luminescence mechanism of the H-CDs. We found that with increasing concentration of the H-CDs in acetic acid medium, initially, the fluorescence intensity gradually increases in the blue region along with a new peak at 465-470 nm possibly due the sub-aggregation of the H-CDs. However, at very high concentration (i.e. 0.5 and 1mg/mL), the emission intensity of the blue end decreases enormously indicating the aggregation-caused quenching (ACQ) of the blue emission. On the other hand, the emission intensity of the H-CDs continuously increases with increasing concentration of the H-CDs.

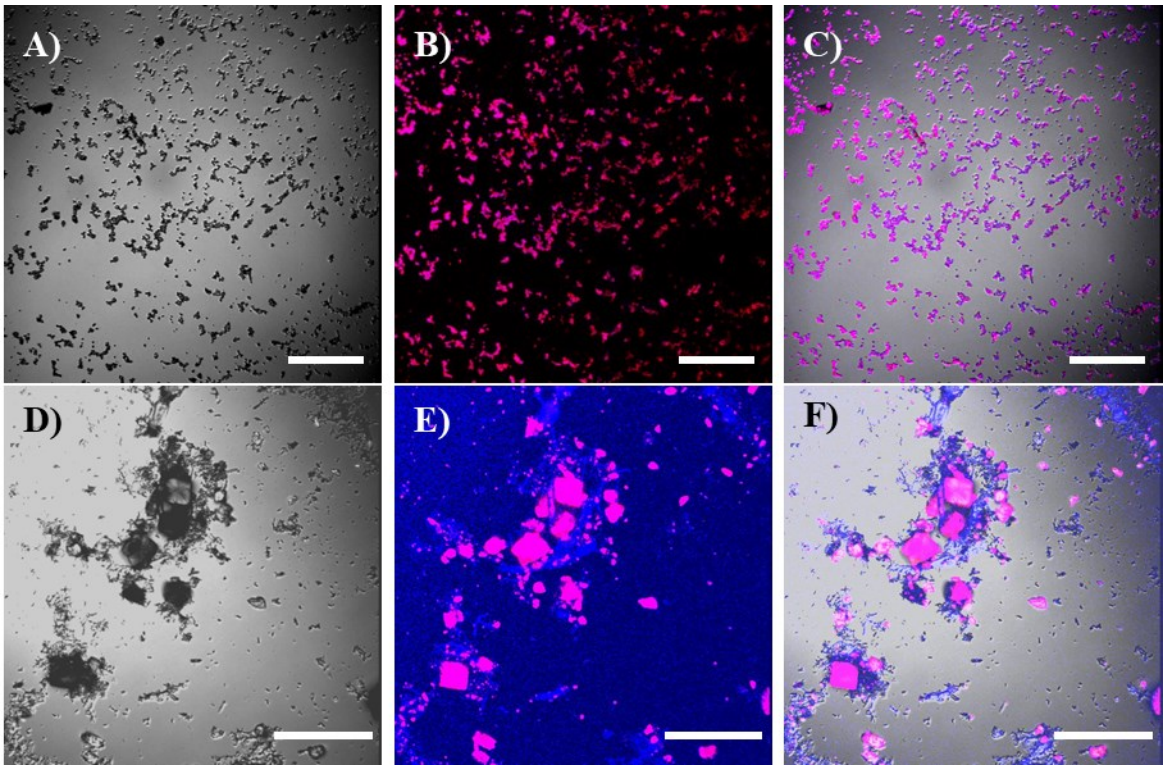

Figure S6: Bright field, confocal, and merge images of the H-CDs in (A-C) ethanol and (D-F) water medium. The scale bar indicates 10 μm.

Discussion: Polarity dependent aggregation of the H-CDs was investigated visually using bright field and confocal microscopy imaging study. We observe that, larger aggregation of the H-CDs in more polar water medium (Figure S6 D-E) compare to the ethanol medium (Figure S6 A-C). Also, the confocal microscopy imaging study reveals that the red emission only generated from the aggregated state of the H-CDs.

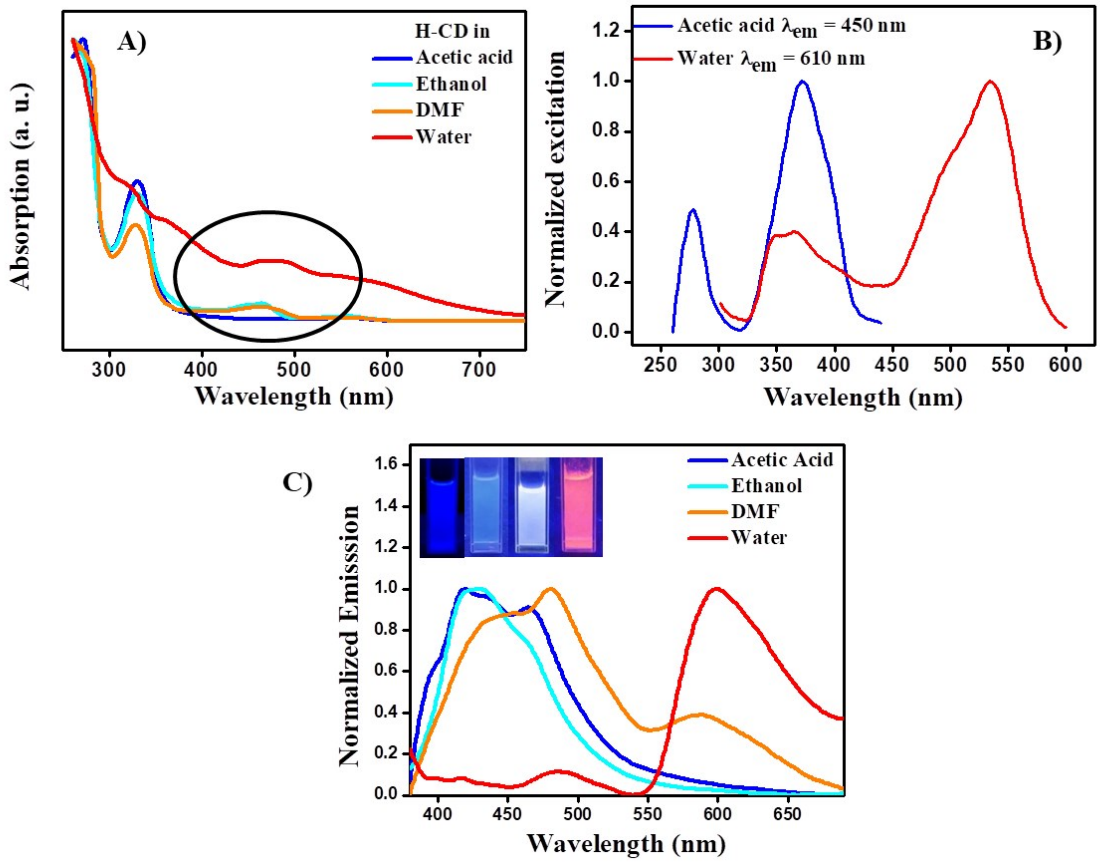

Figure S7: A) UV-Vis absorption spectra, B) normalized excitation and C) Fluorescence emission spectra of the purified H-CDs in different solvents (insets: photographs of the H-CDs in different solvents under 365 nm UV lamp).

Discussion: As shown in **figure S7A**, the H-CDs in acetic acid medium exhibit two peaks at 275 nm and 330 nm which correspond to the π-π* transitions of the C=C in the core of the H-CDs. However, with increasing solvent polarity, we observe decrease in the absorption band at 330 nm with a new peak at 450-500 nm regions, which is attributed to the n-π* transition of the surface states. In aqueous medium, the H-CDs undergo complete aggregation and we observe a broad absorption band at 450-600 nm region. Therefore, with increasing solvent polarity, we observe a gradual decrease at 330 nm and appearance of a new peak at 450-600 nm in absorption band regions.

The above observations are supported by excitation spectra. We observe the H-CDs in acetic acid exhibit a peak at 280 and 360 nm; however in aqueous medium, the H-CDs exhibit a main

peak at 535 nm with a low intensity peak at 360 nm. As mentioned in the manuscript, we observe an increasing red emission with increasing the polarity of the solvent. Therefore, we conclude that the core of the H-CDs is responsible for blue fluorescence and dominant in the non-polar medium, however with aggregation, the blue emission quenches and red emission arises from the surface of the H-CDs in polar medium.

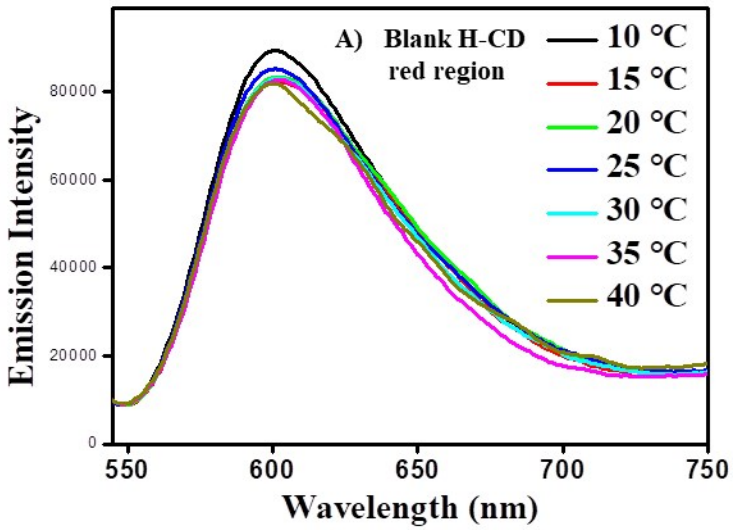

Figure S8: Temperature-dependent emission of the blank H-CD in red region in aqueous medium. Negligible change in fluorescence intensity (~8%) indicates the negligible effect of the temperature on the bare H-CDs red emission.

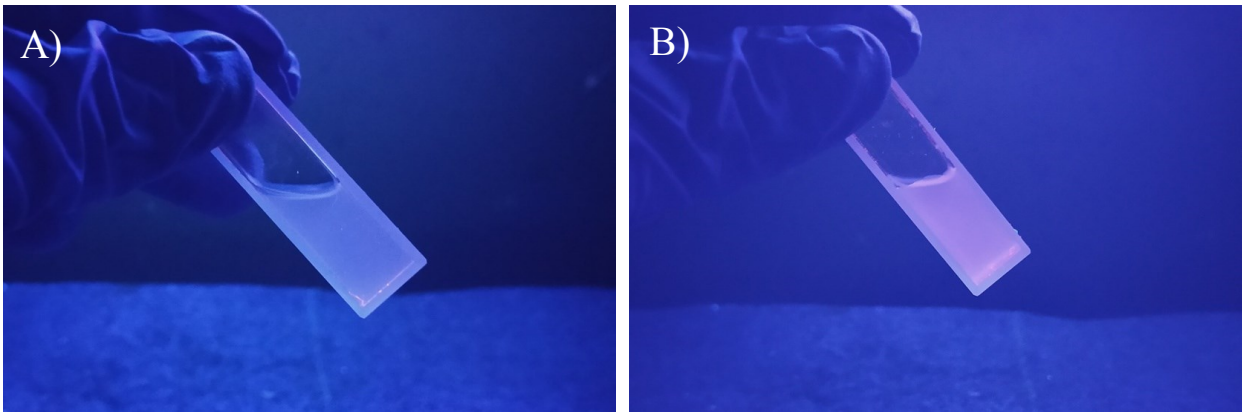

Figure S9: Photographs of the DMPC-CD assemblies at A) 15 °C and B) 35 °C under a 365 nm UV lamp.

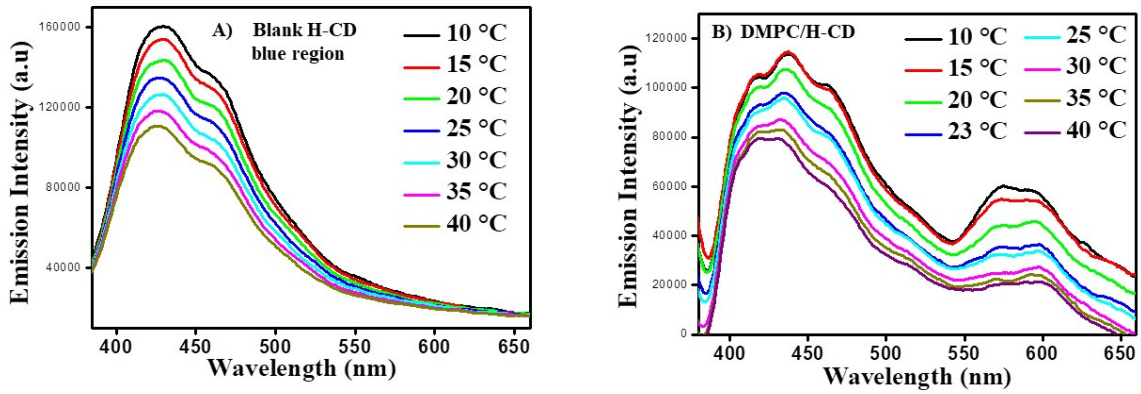

Figure S10: Temperature-dependent emission of the A) blank H-CD in ethanol and B) DMPC/H-CD in blue region upon excitation at 365 nm.

Discussion: We perform the temperature-dependent study of the DMPC-CD assemblies at the blue region (430 nm). We observe a decrease in the emission of DMPC-CD assemblies (~ 28%) with temperature. One may expect that the blue emission of the H-CDs should be increasing with increasing temperature as the phase of the lipid transforms from order phase to disorder phase (reverse phenomena of the red emission region). However, we did not find such observation in the blue emission region. This discrepancy can be explained by the temperature-induced non-radiative transition from the excited state the H-CDs. We observe that the blank H-CDs emission (in ethanol), at the blue region decreases by ~35% with increasing temperature.

Notably, at 40 °C, we observe that the decrease in fluorescence intensity is higher in case of bare H-CDs than lipid-CD assemblies (35% and 28% respectively) which indicates that the lipid bilayer, because of its organization, restricts the non-radiative transition of the H-CDs emission compared to blank H-CDs.

3 Fluorescence property of the other carbon dots with the lipid vesicles:

To prove the uniqueness of the H-CDs used in the present work, we have tested some other CDs which exhibit solvent dependent and aggregation-induced emission property.

Our study reveals that CDs which exhibit the solvent dependent emission or aggregation induced emission do not necessarily show the distinct emission behavior in the different phase states (ordered or disordered state) of the lipid membrane. However, we observe that these CDs generally show little blue shifted emission in lipid membrane from bare CDs emission (in aqueous medium). But till now, there is no report of a CD which exhibit distinct detectable emission under UV lamp or in steady-state fluorescence measurement from both ordered and disordered phase of the lipid (**Figure S11-14**).

The solvent dependent and aggregation induced emission property of the CDs and their emission in the lipid phase state (ordered and disordered phase) are discussed below:

3.1 O-Phenylenediamine (oPD) based carbon dots:

Phenylenediamine is a well-known carbon source for the preparation of the versatile carbon dots (CDs).[2] Therefore, we synthesized oPD-based CDs (o-CDs) by one-step hydrothermal treatment by previously reported procedure.[3] In this context, the choice of CDs is crucial. We choose o-CDs for three reasons, the as-prepared o-CDs is 1) hydrophobic, 2) shows solvent dependent emission, and 3) the emission peak of the o-CDs was sensitive towards water (i. e. o-CDs used to detect water content in organic solvent),[3]. The o-CDs show significant similarities with the photo physical properties with our reported H-CDs.

As reported previously,[3] we found that the as-synthesized o-CD has emission maximum at 570 nm with an excitation spectra at 410 nm in water medium (**Figure S11A**). The o-CD with decreasing solvent polarity exhibit solvent dependent emission spectra which shift gradually from 570 to 512 nm upon excitation at 410 nm (**Figure S11B**), thus resulting in a fluorescence color change from dark yellow to cyan (**Figure S11C**).

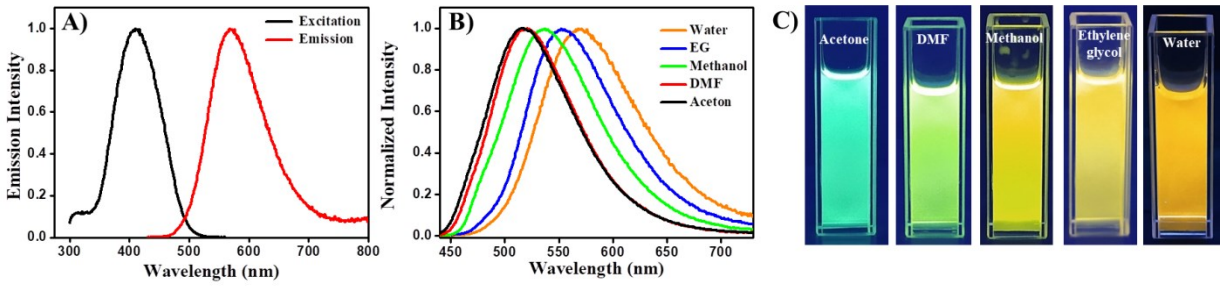

Figure S11: A) Excitation and emission spectra of the o-CD in aqueous solution. B) Solvent-dependent mission spectra of the o-CDs excited at 410 nm and C) their photographs in acetone, DMF, methanol, Ethylene glycol and H_2O under Ultra-Violate lamp.

After checking the excitation dependent emission spectra, the synthesized o-CDs have been used to detect the different membrane phase state. We used thin-film hydration method to prepare the o-CD based lipid-CD assemblies, same as previously used for the H-CDs. We observe that all the lipid-CD assemblies i. e. DOPC-oCD, DMPC-oCD, and DPPC-oCD exhibit 5-7 nm shifted emission from the bare o-CDs emission in aqueous medium (**Figure S12A**). **Figure S12B** shows the photographs of the o-CDs in three different lipids under 365 nm ultraviolet radiations at room temperature and we did not observe significant difference under the UV lamp.

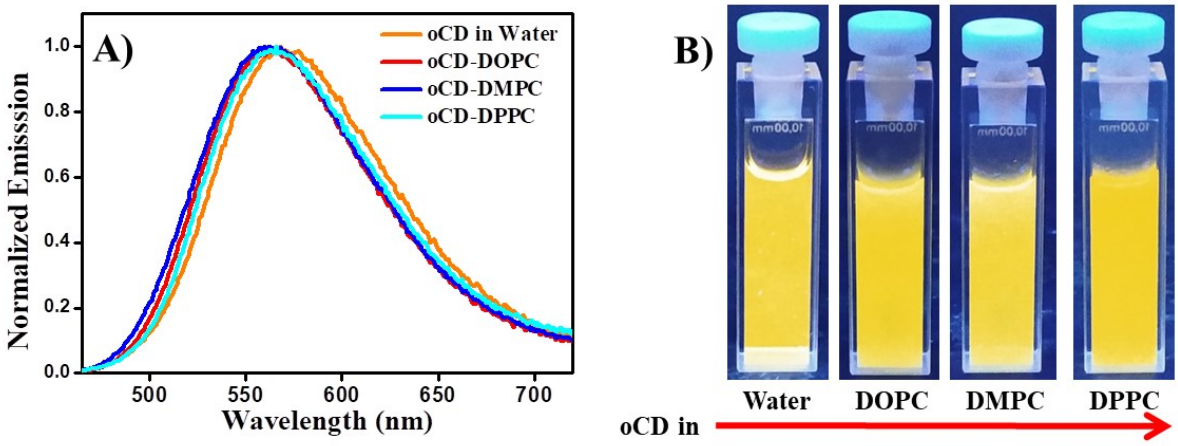

Figure S12: A) Steady-state fluorescence emission spectra (λ_{ex} = 410 nm) and B) the photographs of the o-CDs in DOPC, DMPC and DPPC lipid vesicles under Ultra-Violate chamber.

Therefore, despite of hydrophobic nature of o-CDs and H-CDs, solvent dependent emission, and sensitive emission property towards water, the o-CD does not able to sense the membrane phase behavior. On the other hand H-CDs used in the current work successfully detect different phase state of the lipid membranes.

3.2 Carbon dots synthesized from citric acid and 1-(2-pyridylazo)-2-naphthol:

In this scenario, there is another possibility which cannot be ignored, i. e. the aggregation of the CDs in the bilayer. Aggregation of nanoparticles in the lipid bilayer is well known and it greatly depends on the lipid phase.[5-6] So; one can assume that the CDs possibly undergo the phase dependent aggregation in lipid bilayer by increasing the local concentration and exhibit distinct luminescence in different lipid phases.

Therefore, to investigate the above hypothesis, we need to choose CDs which exhibit the concentration dependent emission i.e. with increasing concentration (and consequently aggregation) the CDs should exhibit different color emission. Therefore, we synthesis another carbon dots, namely M-CDs by solvothermal treatment of citric acid (CA) and 1-(2-pyridylazo)-2-naphthol (PAN) by using a previously reported method **(scheme S4)**.[4] In this case, the M-CD was chosen for its concentration-tunable fluorescence and solvent-dependent emission property (in water and ethanol).

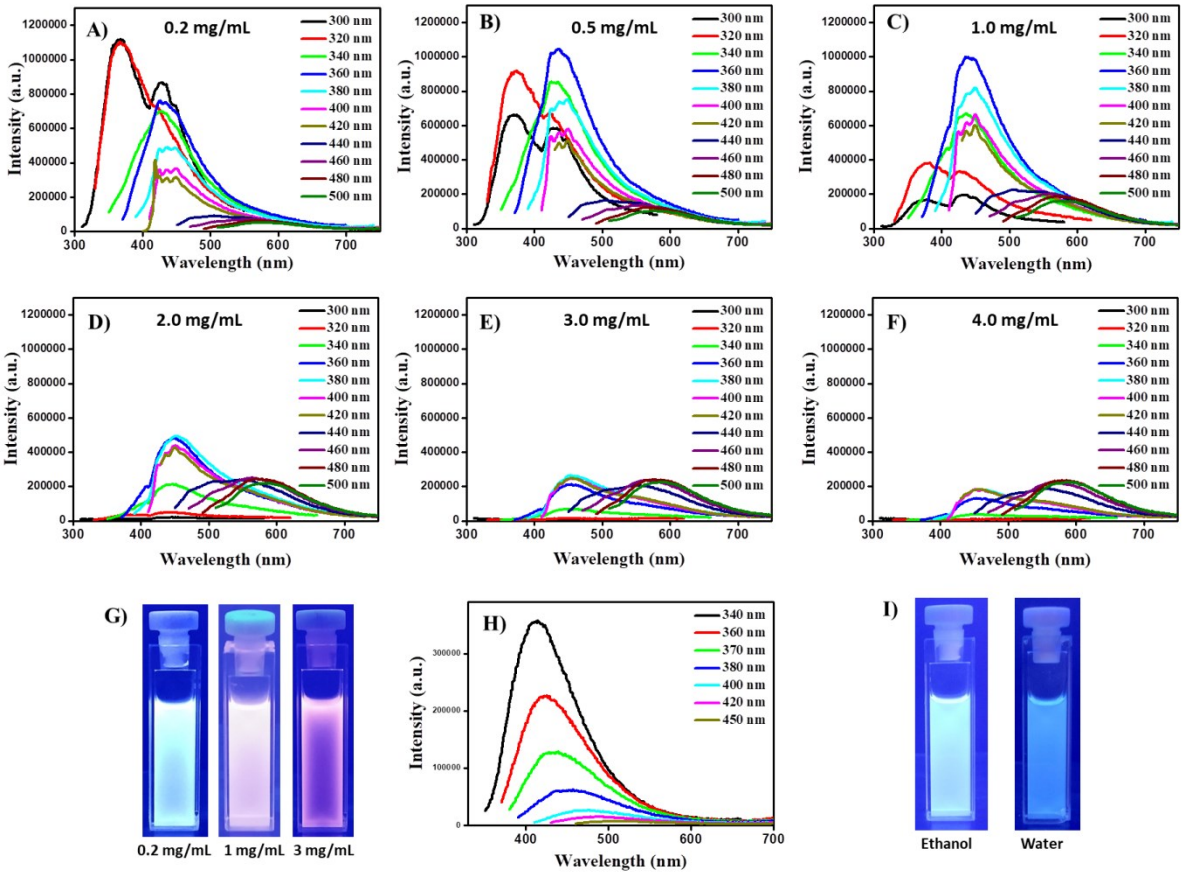

Figure S13: Fluorescence spectra of different concentrations A) 0.2 mg/mL, B) 0.5 mg/mL, C) 1.0 mg/mL, D) 2.0 mg/mL, E) 3.0 mg/mL, and F) 4.0 mg/mL of M-CDs in ethanol solution. We kept the scale bar unaltered for each graph for clear view on concentration dependent quenching. G) Photograph of the different concentration of M-CDs under UV lamp. H) Excitation-dependent emission of the M-CDs in aqueous medium. I) Photograph of the M-CDs (0.5 mg/mL) in ethanol and water medium under UV lamp.

We observed that the synthesized M-CD in ethanol exhibit excitation dependent emission with three main characteristic peak 370 nm, 440 nm and 590 nm when excitation wavelength changes from 300 to 500 nm (**Figure S13B**). Further, the concentration dependent aggregation of the M-CDs was investigated in ethanolic solution using steady state emission spectra (**Figure S13A-F**). We observed that at lower concentration (0.2 mg/mL) H-CD exhibit a main peak at 370 nm; however with increasing concentration (0.5 mg/mL and 1 mg/mL) the peak at 370 nm gradually decreases. On the other hand, the peak at 440 nm gradually increases. When the concentration of the H-CDs is more than 1.0 mg/mL, we observe the peaks at 370 nm and 440 nm decreases and disappear completely with significant emission at 590 nm. The concentration dependent tunable luminescence property of the M-CDs was also observed in the UV chamber (**Figure S13G**). We observed a white emission at lower concentration, however a red emission was observed in high concentration of M-CDs, as reported earlier.[4]The excitation dependent emission of the M-CDs was also measured in water medium (**Figure S13H**). We observe that, in addition to the concentration dependent emission, the M-CD exhibit distinct emission in water (cyan colour) and ethanol (white colour) medium (**Figure S13I**). These photophysical properties of the M-CDs are all accordance with the Yan et. al.[4]

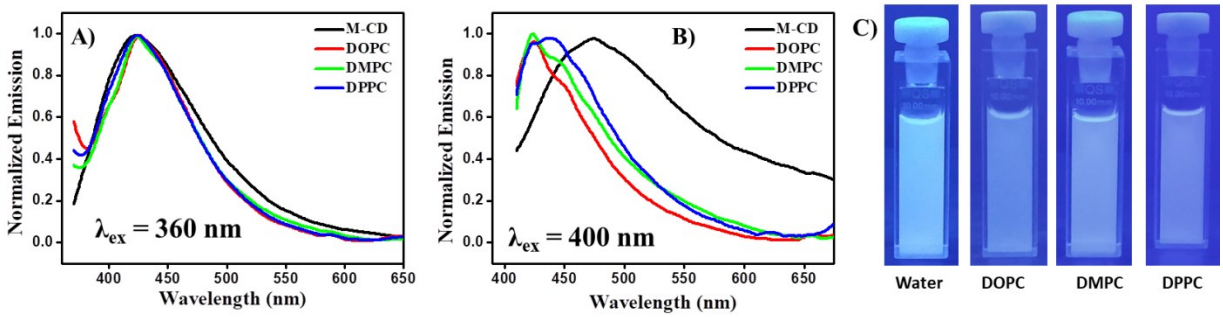

Figure S14: Steady-state emission spectra of the M-CDs in DOPC, DMPC, and DPPC lipid vesicles upon excitation at A) λ_{ex} = 360 nm B) λ_{ex} = 400 nm. C) Photograph of the M-CDs (50 μg/mL) in water and in different lipid vesicles under UV lamp.

Next, we investigated the effect of M-CDs on different phases of the lipid bilayer. We observed that the emission spectra of the M-CDs in aqueous medium do not alter significantly in presence of either order or disorder phase of the lipid upon excitation at 360 nm (**Figure S14D**). Interestingly, upon excitation at 400 nm, M-CDs in lipid vesicles exhibit a huge blue shifted (~120 nm) emission (**Figure S14E)**. However, the spectral shift is almost similar for order and disorder phase of the lipid and above all they do not exhibit significant color differences through naked eyes under UV lamp (**Figure S14F)**. This observation indicates that despite the aggregation possibility of the M-CDs, the M-CDs are not able to detect the different membrane phases. The observation further ascertains the unique ability of the H-CDs of our interest to detect different phases of lipid membrane.

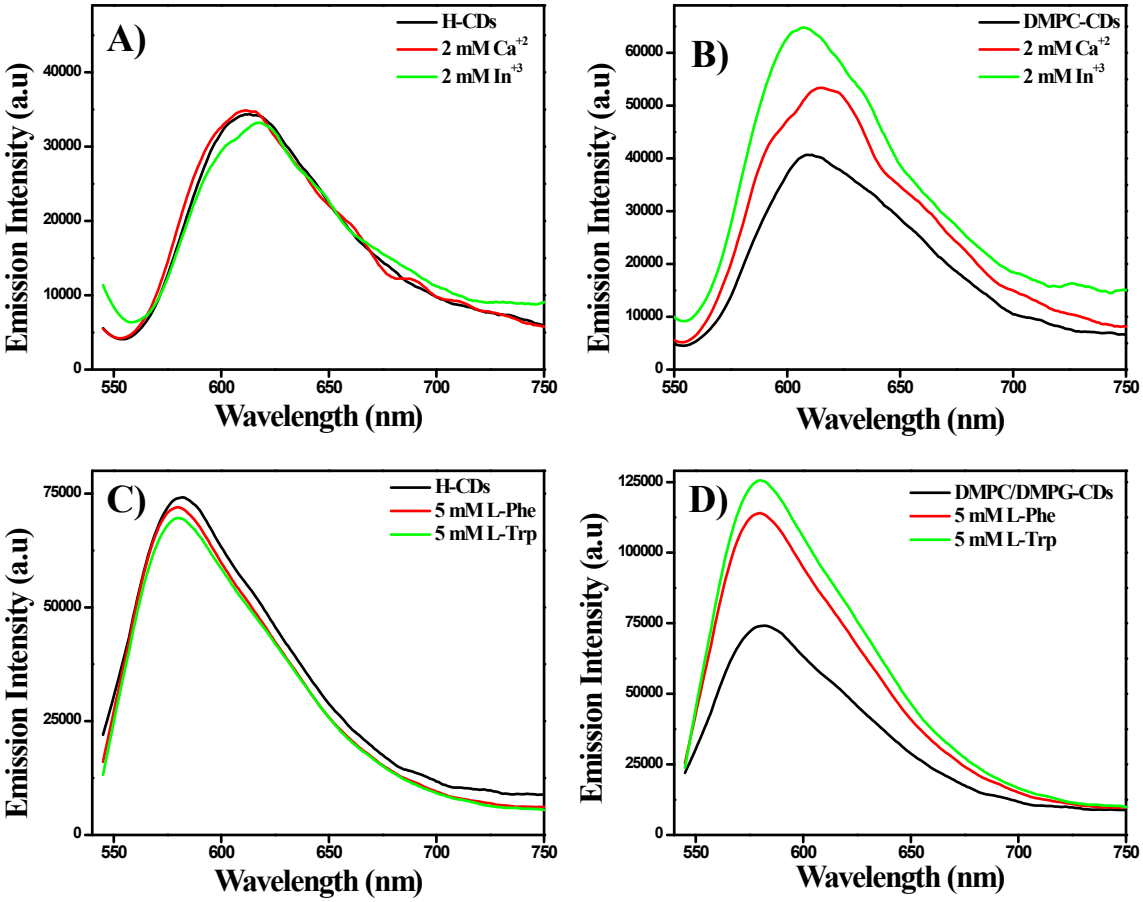

Figure S15: Fluorescence emission spectra of the A) H-CDs and B) DMPC-CD assemblies in presence of 2 mM Ca^{+2} and In^{+3} in water medium. Fluorescence emission spectra of the C) H-CDs and D) DMPC/DMPG-CD assemblies in presence of 5 mM L-Phe and L-Trp in aqueous medium.

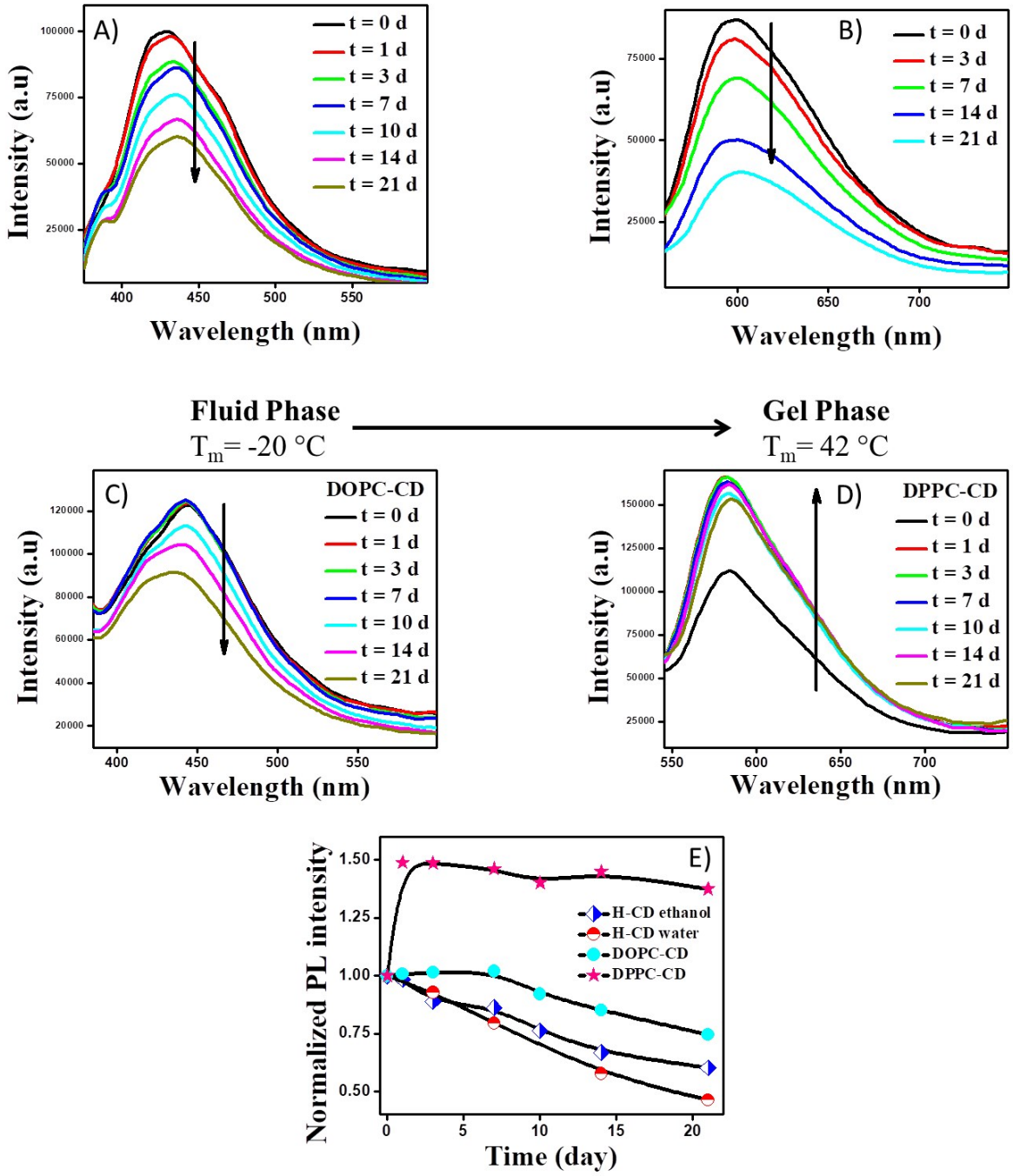

Figure S16: Time-dependent fluorescence emission spectra of the blank H-CDs A) in ethanol, B) in an aqueous medium. Membrane dependent photostability of the lipid-CD assemblies in C) DOPC and D) DPPC. The fluorescence emissions were measure after 0, 1, 3, 7, 10, 14, 21 days upon exposer to ambient light under laboratory condition.

Table S1: Time-resolved lifetime data of DOPC-CDs, DMPC-CDs and DPPC-CDs collected at 600 nm at λ_{ex} = 485 nm at 25 °C.

	χ^2	a_1	a_2	a_3	τ_1	τ_2	τ_3	$<\tau>$
H-CD in water	1.25	0.48	0.33	0.19	0.338	2.25	6.47	2.13
DOPC-CDs	1.02	0.45	0.45	0.10	0.52	2.45	8.47	2.18
DMPC-CDs	1.04	0.37	0.26	0.37	0.54	2.87	7.37	3.6
DPPC-CDs	1.00	0.35	0.30	0.35	0.53	2.70	9.37	4.3

References:

1. H. Yang, Y. Liu, Z. Guo, B. Lei, J. Zhuang, X. Zhang, Z. Liu, C. Hu, Hydrophobic carbon dots with blue dispersed emission and red aggregation-induced emission. *Nat. Commun*. **2019**, *10*, 1789.
2. K. Jiang,S. Sun, L. Zhang,Y. Lu, A. Wu,C. Cai, and H. Lin Red, Green, and Blue Luminescence by Carbon Dots:Full-ColorEmission Tuning and MulticolorCellular Imaging. *Angew.Chem. Int. Ed*. **2015**, *54*, 5360 –5363.
3. D. Chao, W. Lyu, Y. Liu, L. Zhou, Q. Zhang, R. Denga and H. Zhang . Solvent-dependent carbon dots and their applications in the detection of water in organic solvents.*J. Mater. Chem. C* **2018**, *6*, 7527-7532.
4. F. Yan, Y. Jiang, X. Sun, J. Wei, L. Chen, and Y. Zhang. Multicolor carbon dots with concentration-tunable fluorescence and solvent-affected aggregation states for white light-emitting diodes. *Nano Research* **2020**, *13*, 52-60.
5. Wang, F.; Liu, J. Self-Healable and Reversible Liposome Leakage by Citrate-Capped Gold Nanoparticles: Probing the Initial Adsorption/Desorption Induced Lipid Phase Transition. *Nanoscale* **2015**, *7*, 15599−15604.
6. Wang, F.; Curry, D. E.; Liu, J. Driving Adsorbed Gold Nanoparticle Assembly by Merging Lipid Gel/Fluid Interfaces. *Langmuir* **2015**, *31*, 13271−13274.